

# Analysis of a Single Stage Three Level Converter for a Wind Driven Self Excited Induction Generator

Max Savio<sup>1</sup>, Kamal<sup>2</sup>, and Rajesh Kumar<sup>2</sup>

<sup>1</sup> Jeppiaar Institute of Technology/Dept. of Electrical and Electronics Engineering, Chennai, India

Email: maxsavio@jeppiaarinstitute.org

<sup>2</sup> Jeppiaar Institute of Technology/ Dept. of Electrical and Electronics Engineering, Chennai, India

Email: kamalc@jeppiaarinstitute.org, crajeshkumar@jeppiaarinstitute.org

**Abstract**— In this project work, a three phase single stage three level Converter is implemented for a wind energy conversion system. The proposed system is designed for a three phase wind driven Self-Excited Induction Generator (SEIG). The SEIG output is rectified with zero-dead band condition and the output of the converter is continuous. The three level converter is designed and the performance characteristics are studied. The three level converter is operated at a switching frequency of 50kHz to obtain a constant three level output. The proposed model has been simulated in MATALAB Simulink. The hardware prototype model is developed for a lower power rating and the results are compared.

**Index Terms**— Terms—Three Level Converter, Self-Excited Induction Generator (SEIG), Wind Energy Conversion System (WECS), Zero Dead Band.

## I. INTRODUCTION

The demand of power for any application is increasing every day. The renewable energy resources are under considerations since last few years as they are environment friendly. The major fact that the implementation of renewable energy resources like wind energy conversion system [6] requires a conversion techniques for the applications purpose. The power output from the wind energy system using an AC generator probably produced AC output. Based on the requirement the conversion from AD-DC is done using various converters. The main objective is to produce the efficient conversion. This can be possible only by modeling an efficient power converter. The three phase ac-dc power conversion is efficient only when the power factor is correction is performed in the input side so as to apply to various applications. The performance of such converter circuits with input power factor [9]-[10] corrections (PFC) is analyzed using the transformer isolation techniques involving a three phase ac-dc converter and a normal full bridge converter at the load side [1]. The implementation of an AC-DC converter at the supply side and the DC-DC converter at the load side is never been effective economically also, the switching control techniques are more complicated.

Obtaining a cost effective technique with simple control strategies are effective which is explained through a single stage three level converter [2]. The point of obtaining the converter effectiveness with power factor correction could be further implemented in the wind energy conversion technique.

The self-excited induction generator [3] is used as the wind power generator for supplying the power to the converter circuit and thus by achieving the output effectively, the results are discussed. The self-excited induction generator being the fixed speed induction generator has more practical aspects as the experiments conducted using the prime mover characterizes the real time implementation of the wind energy conversion system.

DOI: 01.IJRTET.10.2.7

© Association of Computer Electronics and Electrical Engineers, 2013

The block diagram of the proposed work is shown in the figure 1.

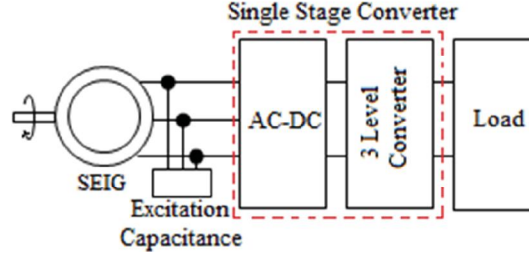


Figure 1. Proposed block diagram

The Self-Excited Induction Generator is operated similar to a wind driven system. The basic modeling of the SEIG with the machine equations is studied for varying wind speed. The output is a three phase which is supplied to the single stage multilevel converter. The single stage [4] multilevel converter has the rectification stage coupled magnetically to the three level dc-dc converters. The power factor correction is performed in the input side through the converter topology and fed to the applications. The performance of the wind driven SEIG is modeled using the values of the excitation capacitance tested practically with varying input conditions.

## II. MODELING OF PROPOSED CONVERTER

The proposed converter consists of the rectification stage coupled magnetically to the three level dc-dc converter. The input AC supply is converted to DC through the rectification and the coupling circuit performs the single stage conversion. The modeling of the proposed converter is shown in the figure 2.

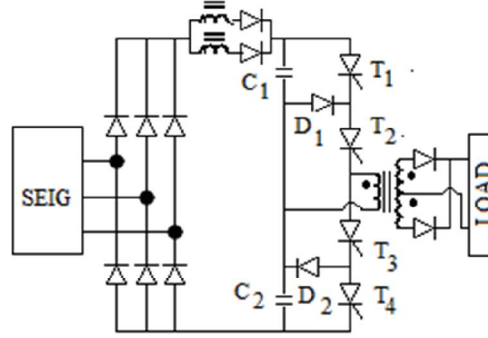


Figure 2. Proposed converter with SEIG

Resonant converters, it can be controlled by varying switching-frequency control, which makes it difficult to optimize their design as they must be able to operate over a wide range of switching frequency. These converters have two conversion stages that allow a portion of the power that is transferred from the input to the output to be processed only once. It is for this reason that they are considered by some to be single-stage converter [7], but they have two converter stages and so have the cost and complexity associated with two-stage converter. Voltage-fed, single-stage, pulse-width modulation converters [8] with a large energy-storage capacitor connected across their primary-side dc bus. The drawbacks of resonant and current-fed converters are not present here. They operate with fixed switching frequency, voltage overshoots and ringing from appearing across the dc bus is prevented by the bus capacitor. Voltage-fed converters have the following drawbacks such as: The primary-side dc bus voltage of the converter may become excessive under high-input-line and low-output-load conditions. The high dc bus voltage results in the need for higher voltage rated devices and very large bulk capacitors for the dc bus. The new voltage-fed converter has more advantages than the conventional converters. The peak voltage stresses of the converter devices is reduced, as the switch voltage is limited to half the dc-bus voltage. It is free from distorted input currents, discontinuous output current, and the use of variable switching frequency. The proposed converter has wide output load variation (from 10% of full load to a full load that is greater than 500 W), PWM control, excellent pf, a

continuous output inductor current, without its components being exposed to excessive peak voltage stresses. The multilevel converter has dc bus voltage which can be split equally among the capacitors so that the capacitors and the converter switches are not exposed to the full dc bus voltage, but are exposed to half of it. This allows greater flexibility in the design of the converter as there is less need to constrain the dc bus voltage. It has greater flexibility in the converter design that allows for improvements in the performance of a single-stage full-bridge converter. The proposed converter is shown in Fig. 2. It consists of an AC input section, a three-level dc-dc converter, and dc link circuitry that is based on auxiliary windings taken from the main power transformer.

### III. MODELING OF SEIG

The Self Excited Induction Generator [3] [5] is modeled based on the electrical machine equation is the reference frame theory. The wind turbine is modeled using the mechanical power equation,

$$P_m = 0.5\rho AC_p v_w^3 \quad (1)$$

Where,  $\rho$  is the air density ( $\text{kg/m}^3$ ),  $A$  is the turbine swept area,  $C_p$  is the performance coefficient of the turbine, and  $v_w^3$  is the wind velocity.

The mechanical power is derived using the performance coefficient which is related to the blade theory and the turbine design. The blade theory gives the relation between the Tip Speed Ratio (TSR) which is given as,

$$C_p = 0.22(116\lambda_i - 0.4\beta - 5)e^{-12.5\lambda_i} \quad (2)$$

$$\lambda_i = \frac{1}{\lambda + 0.08\beta} - \frac{0.035}{1 + \beta^3} \quad (3)$$

Where:  $\beta$  is the pitch angle (degree) and  $\lambda$  is the TSR which is given by,  $\lambda = \omega_m R / V_w$ . From this the mechanical torque is given as,

$$T_m = P_m / \omega_m \quad (4)$$

Where  $\omega_m$  is the rotor angular speed (rad/sec)

The modeling is generally based on the d-q axis equations which is generally represented as in the form of Matrix,

$$\frac{d}{dt} \begin{bmatrix} i_{ds}^e \\ i_{qs}^e \end{bmatrix} = \begin{bmatrix} \frac{-R_s}{L_d} & \frac{L_d P \omega_m}{L_d} \\ \frac{-L_d P \omega_m}{L_q} & \frac{-R_s}{L_q} \end{bmatrix} \begin{bmatrix} i_{ds}^e \\ i_{qs}^e \end{bmatrix} - \begin{bmatrix} \frac{V_{ds}^e}{L_d} \\ \frac{V_{qs}^e - P \omega_m \psi_{pm}}{L_q} \end{bmatrix} \quad (5)$$

Where

$i_{ds}^e$  and  $i_{qs}^e$  are the Stator direct and quadrature current components respectively,

$V_{ds}^e$  and  $V_{qs}^e$  are the direct and the quadrature voltage components respectively,

$R_s$  is the stator resistance,  $L_d$  and  $L_q$  are the direct and quadrature inductance respectively,  $P$  is the number of pole pairs, and  $\psi_{pm}$  is the magnetic flux (weber)

The electromagnetic torque is given by,

$$T_e = \frac{3}{2}P(i_{qs}^e \psi_{pm} + (L_d - L_q)i_{qs}^e i_{ds}^e) \quad (6)$$

From the mechanical equation the electromechanical torque equation is given as,

$$T_m - T_e = J d\omega_m / dt + B \omega_m \quad (7)$$

Where  $J$  is the inertia of the machine and  $B$  is the friction co-efficient.

### IV. CONVERTER OPERATION

During the first stage, switches  $T_1$  and  $T_2$  are ON and energy from the dc-link capacitor  $C_1$  flows to the output load. Since the auxiliary winding generates a voltage that is equal to the total dc-link capacitor voltage (sum of  $C_1$  and  $C_2$ ), the voltage across the auxiliary inductor is the rectified supply voltage. This allows energy to flow from the ac mains into the auxiliary inductor during this mode, and the auxiliary inductor current increases. The supply voltage can be considered to be constant within a switching cycle as the switching frequency is much higher than the line frequency. The current in the auxiliary inductor at the end of this stage is,

$$i_L = \frac{V_{dc}}{L} \quad (8)$$

Where  $V_{dc}$  is the rectified dc voltage,  $L$  is the inductor.

The equation (8) can be represented in terms of Duty cycle and the frequency as,

$$i_L = \frac{V_{dc}}{L} \frac{D}{2f_{sw}} \quad (9)$$

Where D is the duty cycle and  $f_{sw}$  is the switching frequency.

Similarly, the output current which is continuous can be represented as,

$$\Delta i_{L0} = \frac{\left(\frac{V_{dc,avg}}{2N}\right) - V_L}{L_0} * \frac{D}{2f_{sw}} \quad (10)$$

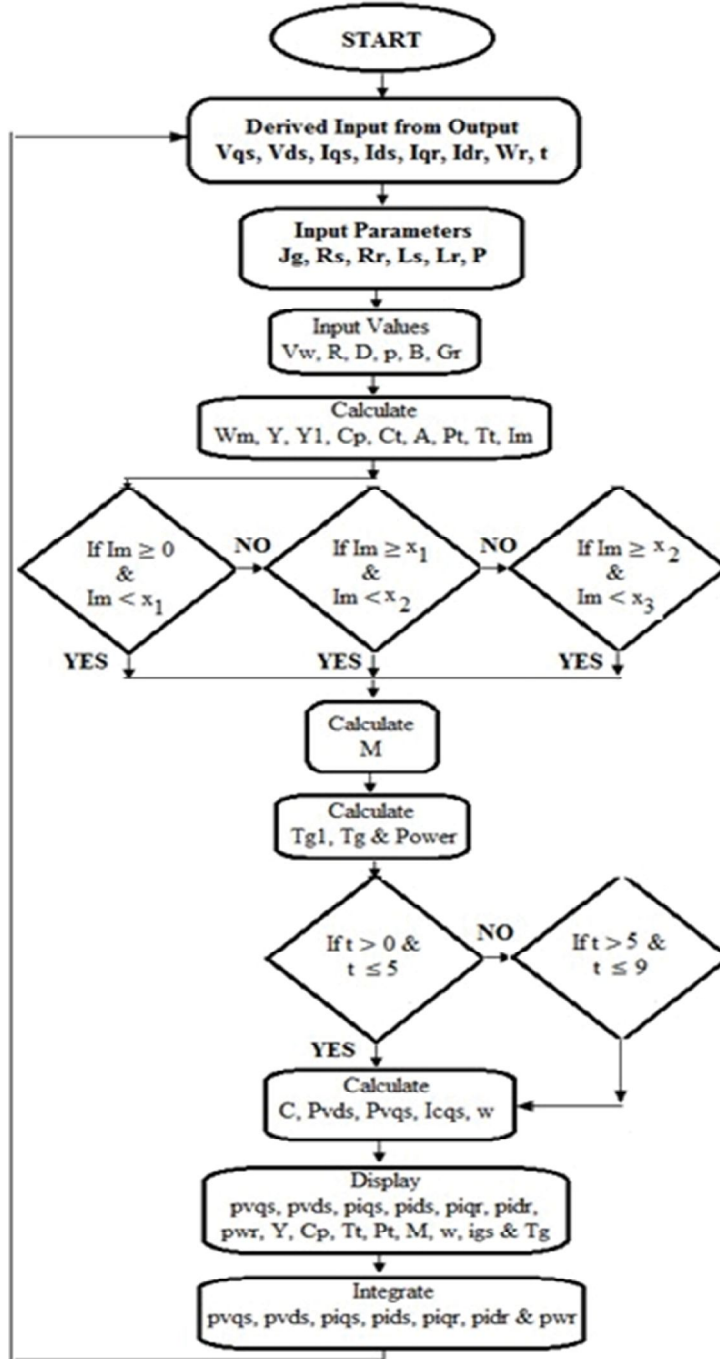


Figure 3. Modeling of Proposed SEIG

## V. SIMULATION AND RESULTS

The proposed system is modeled for the SEIG and the proposed converter using the MATLAB 8. The SEIG is mathematically coded using Matlab program through machine equations. The figure 3 shows the modeling of the SEIG system for the proposed converter.

The modeling consists of the machine input data as the wind turbine input. The  $V_{qs}$ ,  $V_{ds}$ ,  $I_{qs}$ ,  $I_{ds}$ ,  $I_{qr}$ ,  $I_{dr}$ ,  $\omega_r$  and  $t$  are the derived input of voltage and current of the quadrature and direct stator and rotor axis, angular speed respectively. The Input parameters are inertia ( $J_g$ ), stator, rotor resistance ( $R_s$  and  $R_r$ ), stator, rotor inductance ( $L_s$  and  $L_r$ ) and the number of poles ( $P$ ). The physical input data are wind velocity ( $V_w$ ), Rotor radius ( $R$ ), Diameter ( $D$ ) and gear ratio ( $G_r$ ). Using the above data, the Speed, Young's constant, rotor torque and power are determined. The mutual inductance is calculated for the current range based on the required design. The power then extracted are determined through the input derived values.

The values of the excitation capacitance is determined using no load saturation curve of the machine is obtained at normal rated frequency. The voltage source is applied to the stator of the induction machine while its rotor is driven by the DC motor at a constant speed corresponding to the synchronous speed of the machine at 50Hz. It is customarily assumed that the magnetizing current is the difference between stator current and rotor current referred to the stator. In the present case the slip is very small (practically zero) which implies that the magnetizing branch current is essentially measured stator no load current. The no load characteristics of the SEIG as shown in Figure 4. The critical capacitance is limited by the linear region of no load curve, below this value if the capacitance is chosen the voltage will never buildup and excitation fails initially. The minimum capacitance value is limited by the rated voltage of the machine; if we choose below this value the rated voltage will not be generated. The maximum value of capacitance used is limited by the rated motor current. If a capacitance exceeds the maximum value current flow will be more than the rated current which leads to heating of stator core.

The Maximum and the Minimum Capacitance value are calculated for the frequency,  $f = 50\text{Hz}$ . During one switching cycle, the output filter inductor is large enough to assume that the output current is constant and is much greater than resonant inductor  $L_r$ . The capacitor  $C_1$  is large enough to assume that the voltage is constant and ripple free. The boost operation is obtained for the Modulation Index (MI) 0.7 with constant voltage.

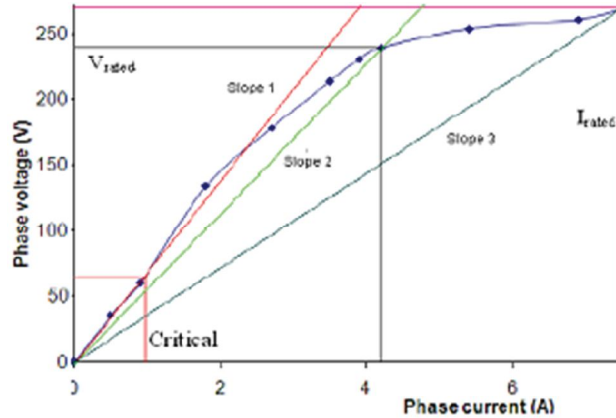


Figure 4. No Load characteristics of SEIG

$X_{cc}$  - Critical capacitive reactance is limited by linear region.

$X_{cmin}$  - Minimum capacitive reactance is limited by rated voltage.

$X_{cmax}$  - Maximum capacitive reactance is limited by rated current.

The simulation results for the 400W wind turbine and the proposed converters are as shown in the figure 5.

## VI. HARDWARE IMPLIMENTATION

The hardware implementation is the prototype model of the proposed system. The hardware is implemented on the converted design using the 40 Pin microcontrollers 8051 for a 230W system. The input voltage is the

three phase supply which is controlled using auto transformer to provide low input voltage and current. The hardware setup is shown in the figure 6.

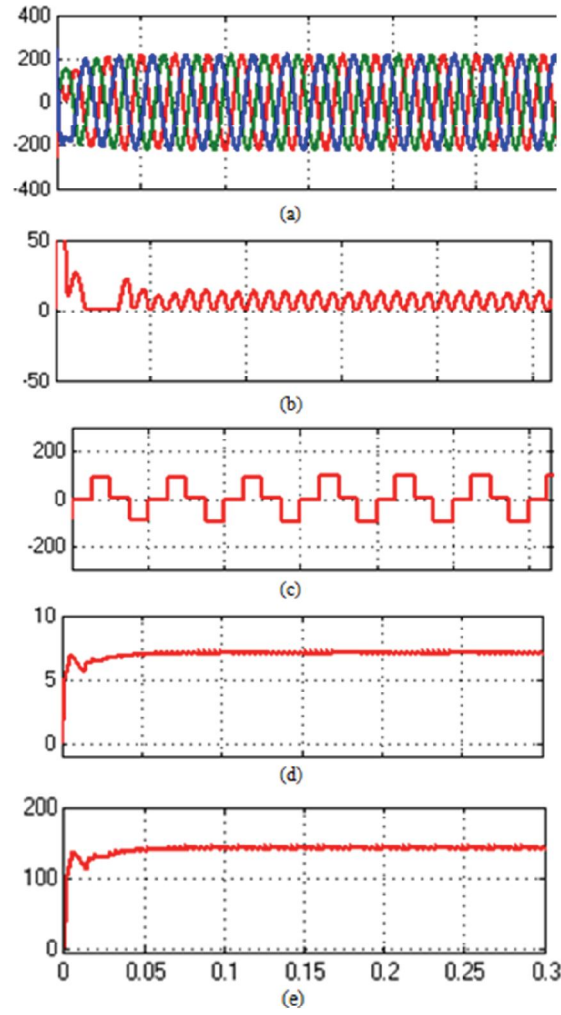


Figure 5. Simulation outputs (a) SEIG phase voltage,  $V_{in}$  (b) Uncontrolled rectifier current,  $I_{dc}$  (c) Inverted output voltage,  $V_s$  (d) Converter output voltage,  $V_{out}$

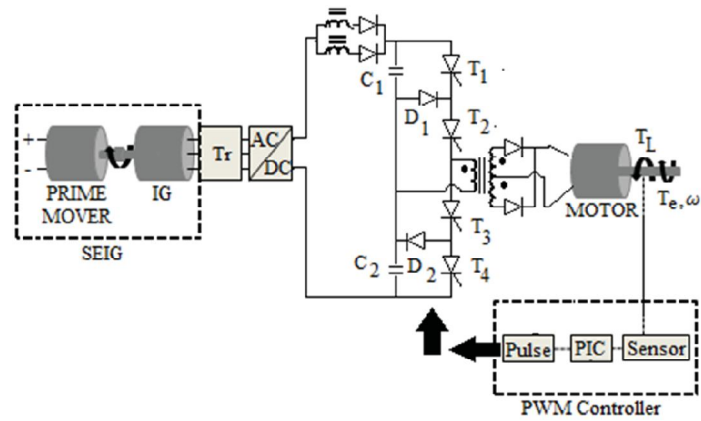


Figure 6. Hardware Prototype model of proposed method

The hardware results are obtained for the different load values. The figure 7 shows the hardware outputs recorded.

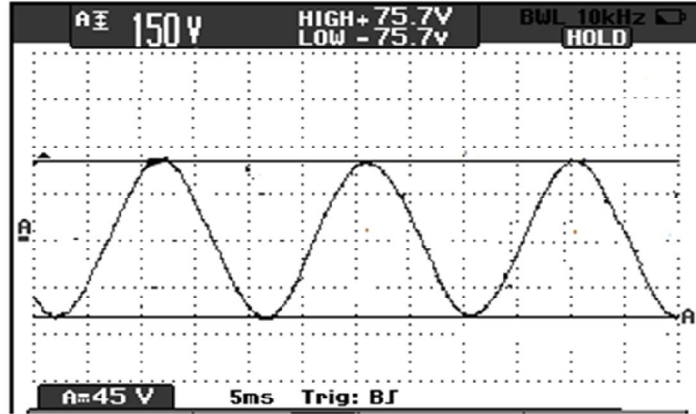


Figure 7. Hardware results of Output Voltage,  $V_{out}$

The output current obtained is 4.1A and the voltage is 45V.

The output values for different load values are determined and the results are discussed as in the table 1

TABLE I. OUTPUT FOR DIFFERENT LOAD VALUES

Load $R(\Omega)$	Voltage (V)	Current (A)
10	46.06	4.60
12	46.41	3.86
14	46.67	3.33
16	46.87	2.93
18	47.03	2.61
20	47.16	2.35

The proposed converter characteristics are shown as in the figure 8.

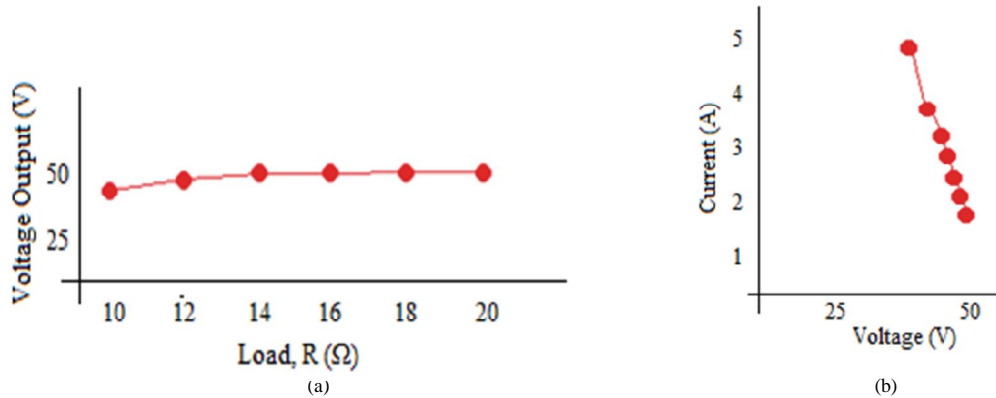


Figure 8. Output characteristics (a) Steady State Characteristics (b) I-V Characteristics

## VII. CONCLUSION

Thus a three-phase, single-stage voltage-fed, three-level, ac/dc converter which operates with a three phase wind driven SEIG system operates.. This converter can operates with a better efficiency and with less output inductor current ripple and universal input voltage and wide load operating range. The results of simulation for conventional and proposed method with R load and hardware implementation is presented and the results



are obtained. The analysis on the output characteristics deliver that the implementation of the wind energy conversion system has greater utility used for the prosed techniques.

#### VIII. ACKNOWLEDGEMENT

The authors thank the Director, Dr. N Marie Wilson, Jeppiaar Institute of Technology, Chennai, India for providing technical and financial support for the research work. The authors also thank the Dept. of Electrical and Electronics Engineering, Jeppiaar Institute of Technology for providing a technical support in hardware development.

#### REFERENCES

- [1] Mehdi Narimani and Gerry Moschopoulos (2013), "A Novel Singe Stage Multilevel Type Full Bridge Converter.", IEEE Trans. on Industrial Electronics, Vol. 60, No. 1, pp. 31-43.
- [2] P. D. Ziogas, Y. Kang, and V. R. Stefanovic, (1985) "PWM control techniques for rectifier filter minimization," IEEE Trans. Ind. Appl., vol. IA-21, no. 5, pp. 1206-1214.
- [3] Sasikumar M. and Chenthur Pandian S.(2010), "Performance characteristics of self - excited induction generator fed current source inverter for wind energy conversion system," International Journal of Computer and Electrical Engineering (IJCEE), Vol. 2, No. 6, pp. 1077-1080.
- [4] J. M. Kwon, W. Y. Choi, and B. H. Kwon (2011), "Single-stage quasi-resonant flyback converter for a cost-effective PDP sustain power module," IEEE Trans. Ind. Electron., vol. 58, no. 6, pp. 2372-2377.
- [5] Max Savio and Sasikumar M (2012), "Space Vector Control Scheme of Three Level ZSI Applied to Wind Energy System," International Journal of Engineering (IJE) ,Vol 25, No. 2. pp 392-402.
- [6] F Max Savio and Sasikumar M (2012), "An Effective Control Technique for an Impedance Source Inverter based Wind Energy System", IEEE Conference Proceedings of Emerging Trends in Electrical and Energy management (ICETEEEM), pp. 404-410.
- [7] H. S. Ribeiro and B. V. Borges (2010), "Analysis and design of a high-efficiency full-bridge single-stage converter with reduced auxiliary components," IEEE Trans. Power Electron., vol. 25, no. 7, pp. 1850-1862, Jul. 2010.
- [8] S. K. Ki and D. D.-C. Lu (2010), "Implementation of an efficient transformer-less single-stage single-switch ac/dc converter," IEEE Trans. Ind. Electron., vol. 57, no. 12, pp. 4095-4105.
- [9] H. J. Chiu, Y. K. Lo, H. C. Lee, S. J. Cheng, Y. C. Yan, C. Y. Lin, T. H. Wang, and S. C. Mou (2010), "A single-stage soft-switching flyback converter for power-factor-correction applications," IEEE Trans. Ind. Electron., vol. 57, no. 6, pp. 2187-2190.
- [10] J. Zhang, D. D.-C. Lu, and T. Sun (2010), "Flyback-based single-stage power factor-correction scheme with time-multiplexing control," IEEE Trans. Ind. Electron., vol. 57, no. 3, pp. 1041-1049.